Studies on the Power Requirement of Mixing Impellers (I) : Liquid Flow and Power Requirement for Paddle Agitators in Cylindrical Vessels

AUTHOR(S):

NAGATA, Shinji; YOSHIOKA, Naoya; YOKOYAMA, Tōhei

CITATION:

NAGATA, Shinji ...[et al]. Studies on the Power Requirement of Mixing Impellers (I) : Liquid Flow and Power Requirement for Paddle Agitators in Cylindrical Vessels. Memoirs of the Faculty of Engineering, Kyoto University 1955, 17(3): 175-185

ISSUE DATE:

1955-08-15

URL:

http://hdl.handle.net/2433/280329

Studies on the Power Requirement of Mixing Impellers (I)

—Liquid Flow and Power Requirement for Paddle Agitators in Cylindrical Vessels.—

By

Shinji NAGATA, Naoya YOSHIOKA and Tōhei YOKOYAMA

(Department of Chemical Engineering)

(Received April, 1955)

The following studies were carried out concerning the angular velocity distribution of the liquid in a cylindrical vessel agitated by a concentric paddle agitator.

In such cases, the flow pattern in a vessel is similar to that of the so called Rankine's combined vortex. The Liquid near the center of a vessel, rotates with the same angular velocity as that of the agitator (forced vortex part), and in the outer part, the flow is similar to that of free vortex motion in which the rotating velocity of liquid is inversely proportional to the distance from the center of rotation (free vortex part). If the above velocity distribution is assumed, the predicted shape of liquid surface contours shows fair agreement with the observed data.

Also, by measuring the agitator power requirements, the radius of the forced vortex was evaluated.

Then, the rate of increase in power requirements accompanied by the increase in paddle width was reasonably explained by these theories.

I. Theoretical considerations on the state of liquid flow and the liquid surface contour.[1]

Although the condition of liquid flow which is brought about by concentric agitators in cylindrical vessels is very complex, the following rough approximations are proposed.

In a cylindrical vessel (r_2 in radius, H in static liquid depth as shown by Fig. 1a) a

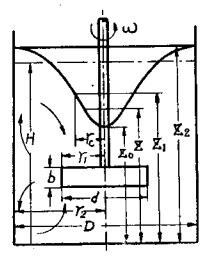

Fig. 1 a. Agitation Vessel and Notations Used.

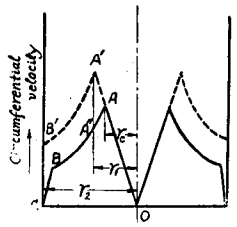

Fig. 1 b. Circumferential Velocity Distribution of Liquid in an Agitated Vessel.

flat rectangular paddle agitator $2r_1$ in length and b in width is installed vertically, which rotates at an angular velocity ω. If the viscosity of liquid were insignificant and the friction at the wall and bottom were negligible, the liquid in the central zone of radius r_1 would rotate at an angular velocity equal to that of the paddle like a solid cylinder. But in reality, there exists friction at the wall surface, therefore the radius r_c of the cylindrically rotating zone is smaller than the radius r_1 of the paddle and in the outer zone where $r>r_c$, the circumferential velocity distribution of the liquid resembles that of a free vortex. Thus,

$$r \leqq r_c \quad ; \quad v = r\omega \tag{1}$$

v increases linearly as shown by the straight line OA in Fig. 1b. This region is called the forced vortex where the resultant of centrifugal force $mr\omega^2$ and gravity force mg balances with the increase in static pressure, and is in almost stationary state relative to the paddle.

The free surface of the liquid in this zone is a sort of isobaric and is a rotating parabola as is generally known.

$$dz/dr = mr\omega^2/mg \tag{2}$$

The relationship between z_0, the liquid depth at the center and z, the liquid depth at a distance r from the center line is derived by integrating equation (2).

$$r \leqq r_c \quad ; \quad z = z_0 + (\omega^2 r^2/2g) \tag{3}$$

Then, in the free vortex zone the circumferential velocity is inversely proportional to the radius of the curvature of a stream-line, thus:

$$r \geqq r_c \quad ; \quad vr = \text{constant} \tag{4}$$

In general, a compound vortex motion has been wellknown for a long time and is now called Rankine's combined vortex[2),3),4)].

On a transitional cylindrical surface between two types of flow, both equations (1) and (4) hold.

$$vr = r_c^2\omega \tag{4'}$$

Therefore, in the region where $r \geqq r_c$

$$v = r_c^2\omega/r \tag{4''}$$

This relation is shown as a hyperbolic velocity distribution curve AB in Fig. 1b. In this region, the following relations hold and the equation (5) showing the surface contour is derived.

$$\left.\begin{aligned} z+\frac{v^2}{2g} &= z+\frac{\omega^2 r_c^4}{2gr^2} = z_1+\frac{\omega^2 r_c^2}{2g} \\ r \geqq r_c \quad ; \quad z &= z_1+\frac{\omega^2 r_c^2}{2g}\left(1-\frac{r_c^4}{r^2}\right) = z_0+\frac{\omega^2 r_c^2}{2g}\left(2-\frac{r_c^2}{r^2}\right) \end{aligned}\right\} \quad (5)$$

This is a sort of equation for hyperbola. In the above discussion, it has been assumed that the point A represents a sharp boundary, but in reality there may be a transitional range and the state of flow changes gradually. Accordingly the equation (5) may not hold good in this region. Moreover, the flow pattern in a steady state of agitation is not a simple curvilinear flow confined in a horizontal direction, but there are circulating currents, discharged radially by the paddle and separated at the wall surface into upward and downward flows, returning to the paddle passing through the central zone of the vessel as shown in Fig. 1a.

Nevertheless, it can be proved that the above theory is valid as a rough approximation by the facts that surface contour calculated by equations (3) and (5) agrees comparatively well with the shape observed as shown by Fig. 3.

On the side wall of a vessel, a stationary film is formed and the velocity of the liquid near the wall is derived by substituting r_2 for r in equation (4).

$$v = r_c^2\omega/r_2 \quad (6)$$

Between this layer and the wall surface, there is a sudden velocity decrease as shown by BC in Fig. 1b.

Of course, there may be differences in circumferential velocities in the vertical direction.

As a result of this rotational flow, the liquid surface in the central zone becomes depressed, and the liquid level z_2 at the wall becomes higher as the rotational speed increases. Hence,

$$z_2 = z_0+\frac{\omega^2 r_c^2}{2g}\left(2-\frac{r_c^2}{r_2^2}\right) \quad (7)$$

Now, taking the total liquid volume as V and the static liquid level as H, then,

$$H = V/\pi r_2^2 \quad (8)$$

and in rotating condition,

$$\begin{aligned} V &= \int_0^{r_c}\left(z_0+\frac{\omega^2 r^2}{2g}\right)2\pi r dr+\int_{r_c}^{r_2}\left\{z_0+\frac{\omega^2 r_c^2}{2g}\left(2-\frac{r_c^2}{r^2}\right)\right\}2\pi r dr \\ &= z_0\pi r_2^2+\frac{\pi\omega^2}{4g}r_c^4+\frac{\pi\omega^2}{g}r_c^2(r_2^2-r_c^2)-\frac{\pi\omega^2 r_c^4}{g}\ln\left(\frac{r_2}{r_c}\right) \end{aligned} \quad (9)$$

Now, let r_c/r_2 be denoted as $y\ (\leqq 1)$ and substituting the relation of equation (8) for equation (9), the following equation is derived.

$$\left(\frac{H-z_0}{r_2^2}\right)\left(\frac{g}{\omega^2}\right) = y^2 - y^4\left\{2.303\log\left(\frac{1}{y}\right)+\frac{3}{4}\right\} \tag{10}$$

or

$$z_2 = H+\frac{\omega^2}{g}r_2^2y^2\left\{\frac{1}{4}+2.303\log\left(\frac{1}{y}\right)\right\} \tag{11}$$

The values of $\{(H-z_0)/r_2^2\}(g/\omega^2)$ which can be calculated by observed values of z_0 and ω, are functions of y only. If the values of the right-hand side of equation (10) are calculated beforehand for various values of y and plotted against $y=0\sim1$ as shown in Fig. 2, then from the calculated values for the left-hand side of equation (10), values of y or r_c can be determined in regard to

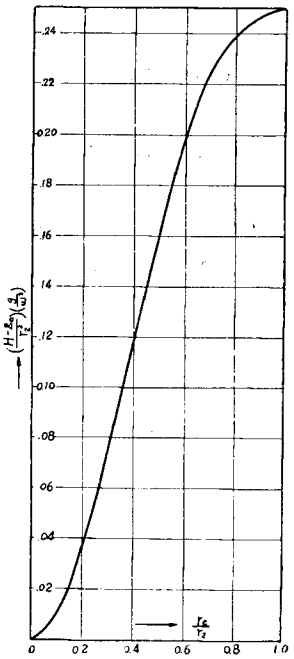

Fig. 2. Diagram Showing Estimation of y or r_c from Liquid Surface Contour.

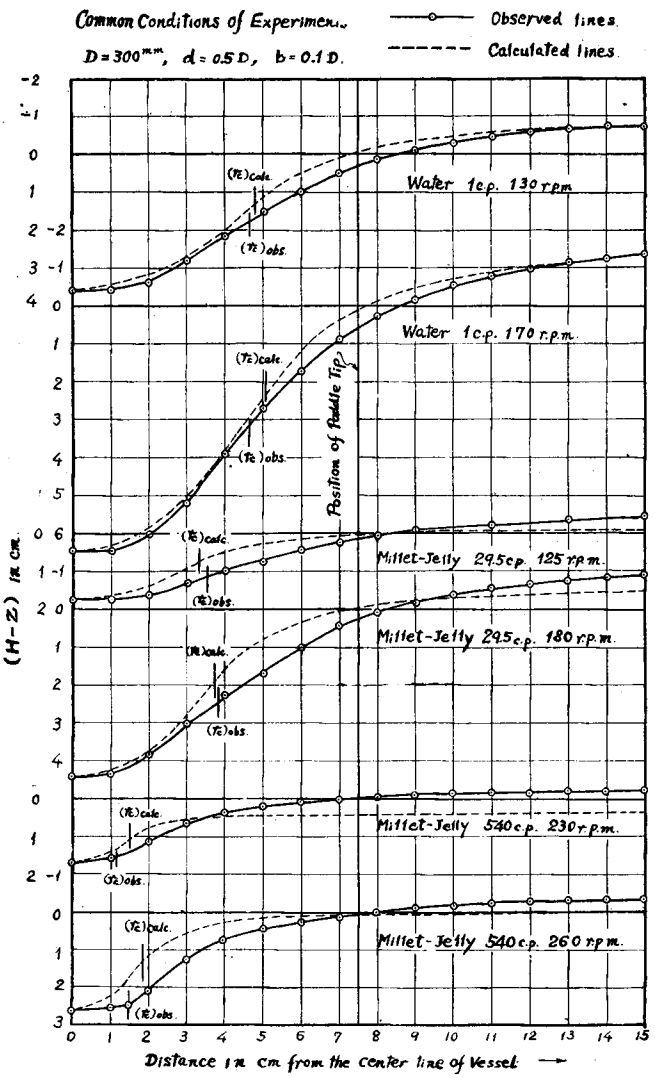

Fig. 3. Comparisons of the Observed Liquid Surface Contours with those Calculated by Equations (3) and (5).

various agitation conditions. These values of r_c are very important in determining the states of liquid flow in the vessels.

In Fig. 3, the experimentally determined liquid surface contours (solid lines) are compared with those calculated by equations (3) and (5) (dotted lines). In these experiments, paddle used has a dimension of $d=0.5D$, $b=0.1D$ and the viscosities of liquids agitated by the paddle vary widely from 1 c.p. to 540 c.p.. Comparatively good agreements are found in these experiments. But in cases of other paddles, deviations between calculated and observed curves are large, especially in the case of paddles with large d/D and b/D ratios, so that the above theory has a limited range of application.

II. The size of the cylindrical rotating zone and power consumption.[5]

As mentioned above, the liquid in the cylindrically rotating zone is revolving with the same angular velocity as that of paddle. Therefore, the mixing efficiency of this zone is low. Although the size of the cylindrically rotating zone (forced vortex zone) can be determined by the liquid surface contour as mentioned above, another method is proposed as shown in Fig. 4.

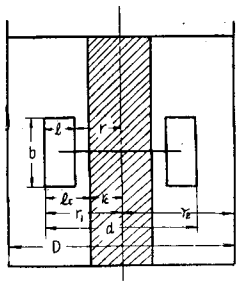

Fig. 4. Schematic Diagram of Impellers Used for the Determination of the Size of Cylindrically Rotating Zone.

Power consumptions for impellers equal in d and b but with various width l were measured and the ratio of the power to the power for a paddle (P_{paddle}) is shown in Fig. 5 as ordinate with l/r_1 as abscissa.

Any increase in l results in the increase in power until finally l reaches $l_c\,(=r_1-r_c)$ where power consumption for impellers reaches a maximum and equals that of the paddle.

Fig. 6 is a diagram for the explanation of power consumptions. The paddle rotates with a linear velocity OAA' and the liquid flows with a velocity OAA'' so that the outer part of the paddle of length l_c contributes to the power consumption while the inner part of length r_c does not.

An element of area bdl collides with liquid at a relative velocity $u_r=\overline{ab}$ so that the resisting force df is,

$$df = K\rho u_r^2 bdl \tag{12}$$

When the impeller rotates opposing to this resisting force at a relative velocity u_r, the power consumption P is

$$P=\int_0^l K\rho u_r^3 bdl \quad (l=r_1-r) \tag{13}$$

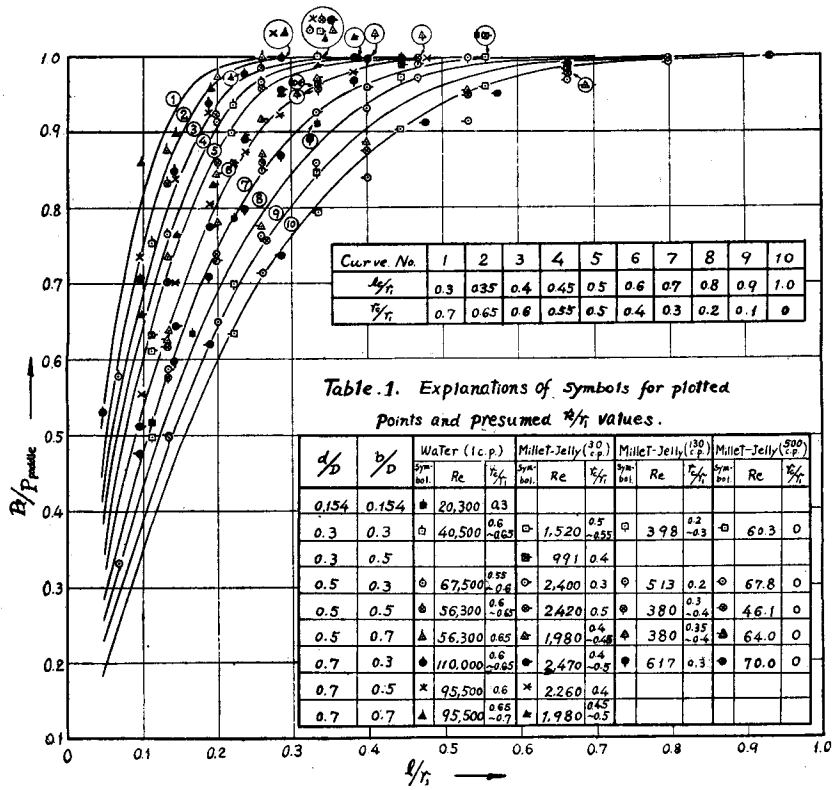

Table. 1. Explanations of Symbols for plotted Points and presumed r_2/r_1 values.

d/D	b/D	Water (1 c.p.) Sym-bol.	Re	r_2/r_1	Millet-Jelly (30 c.p.) Sym-bol.	Re	r_2/r_1	Millet-Jelly (130 c.p.) Sym-bol.	Re	r_2/r_1	Millet-Jelly (500 c.p.) Sym-bol.	Re	r_2/r_1
0.154	0.154	●	20,300	0.3									
0.3	0.3	□	40,500	0.6~0.65	□	1,520	0.5~0.55	□	398	0.2~0.3	□	603	0
0.3	0.5				■	991	0.4						
0.5	0.3	⊙	67,500	0.55~0.6	⊙	2,400	0.3	⊙	513	0.2	⊙	67.8	0
0.5	0.5	◆	56,300	0.6~0.65	◆	2420	0.5	◆	380	0.3~0.4	◆	46.1	0
0.5	0.7	▲	56,300	0.65	▲	1,980	0.4~0.45	▲	380	0.35~0.4	▲	64.0	0
0.7	0.3	●	110,000	0.6~0.65	●	2,470	0.4~0.5	●	617	0.3	●	70.0	0
0.7	0.5	×	95,500	0.6	×	2,260	0.4						
0.7	0.7	▲	95,500	0.65~0.7	▲	1,980	0.45~0.5						

Fig. 5. Diagram to Estimate the Radius r_c of Cylindrically Rotating Zone for Liquids of Various Viscosities.

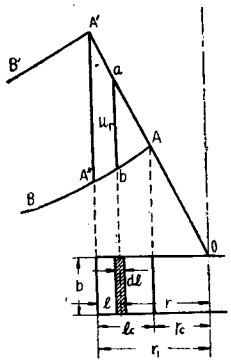

Fig. 6. Diagram Showing Relative Velocity Distribution between Paddle and Liquid.

If the line AA'' is approximated as a straight line, and K as a constant for convenience' sake, then the relative velocity is equal to $c\,(l_c-l)$ and the following relation is derived, where K' is equal to KC^3.

$$P_l = KC^3\rho\int_0^l (l_c-l)^3\,dl = (K'/4)\,\rho\{l_c^4-(l_c-l)^4\} \quad (14)$$

When $l=l_c$, $P=(K'/4)\,\rho l_c^4$ and this power is equal to P_{paddle}, therefore,

$$\frac{P_l}{P_{\text{paddle}}} = \frac{l_c^4-(l_c-l)^4}{l_c^4} \quad (14')$$

$$\frac{P_l}{P_{\text{paddle}}} = \frac{(l_c/r_1)^4-(l_c/r_1-l/r_1)^4}{(l_c/r_1)^4} \quad (14'')$$

Curve (10) in Fig. 5 is a calculated line, assum-

ing $r_c=0$, in other words the cylindrically rotating zone has disappeared. Then $u_r=c'(r_1-l)$ for varying l.

$$P_l=K''\rho\int_0^l(r_1-l)^3\,dl=(K''/4)\,\rho\{r_1^4-(r_1-l)^4\} \tag{15}$$

Substituting $l\doteqdot r_1$ in equation (15), the power consumption of a paddle is obtained.

$$\frac{P_l}{P_{\text{paddle}}}=\frac{r_1^4-(r_1-l)^4}{r_1^4} \tag{15'}$$

Of course, if the length l is smaller than l_c, the velocity distribution will be found different from that of a paddle having equal dimensions in d and b. As a rough approximation, the differences due to the variations of l_c are shown by curves (1), (2), ··· (9), (10) in Fig. 5.

The observed values of (P_l/P_{paddle}) for various values of l, fall on the lines (1) to (10) in Fig. 5. Plotted data points and calculated lines do not agree well, especially in the ranges where (P_l/P_{paddle}) values are dislocated from 1.0 due to the approximations mentioned above. However by proper selections and interpolations, values of (l_c/r_1) or (r_c/r_1) can be determined in regard to the liquids of various viscosities.

Several results are shown in Table 1 which are inserted in the lower half of Fig. 5.

The values of r_c determined by this method are marked in Fig. 3 by the lines noted as $(r_c)_{\text{obs}}$. Also the values of r_c calculated by the equation (10) or by Fig. 2 are marked by the lines noted as $(r_c)_{\text{calc}}$. These two values of r_c agree fairly well in the case of this example ($d=0.5D$, $b=0.1D$). But for paddles with large ratios in d/D, e. g. $d/D=0.7$, the agreement is not always good. However it may be concluded that the value of r_c becomes smaller with the increases in the viscosities of agitated liquids.

Upper curve in Fig. 7 shows the (r_c/r_1) values plotted against the Reynolds number $(d^2n\rho/\mu=d^2\omega\rho/2\pi\mu)$.

Excepting the case of $d/D=0.154$, values of (r_c/r_1) take a nearly constant value ranging from 0.6 to 0.65 for the Reynolds number above 4×10^4 and drop off suddenly below the Reynolds number of 2,000.

When $R_e/(r_c/r_1)$ is plotted versus R_e, a straight line is obtained as shown in the lower half of Fig. 7 and the following relation is obtained.

$$\frac{r_c}{r_1}=\frac{R_e}{10^3+1.6R_e} \tag{16}$$

The effects of paddle length (d/D) and paddle width (b/D) on the ratio (r_c/r_1) are not conclusive from these experiments, but there is indication that (r_c/r_1) becomes smaller as the ratio (d/D) becomes considerably smaller.

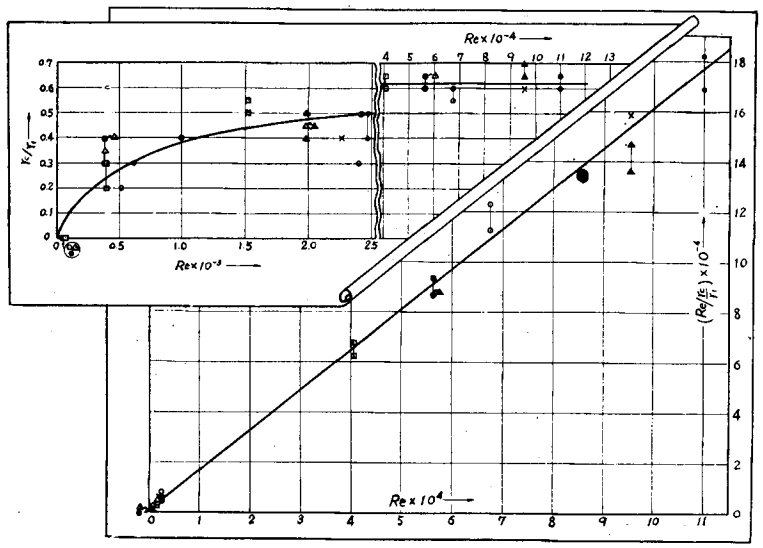

Fig. 7. Diagram Showing (r_c/r_1) versus Reynolds Number.

It will then be concluded that the size of the cylindrically rotating zone (r_c/r_1) approaches zero when the Reynolds number is lowered and tends to 100. In other words, the total areas of the paddle are exposed to flow resistance and the maximum power $(P_{max.})_1$ for this paddle is attained.

When the vessel diameters are increased holding the paddle size constant, the cylindrically rotating zones become smaller and smaller in the same way as when viscosities increased. The power consumptions increase to a maximum value $(P_{max.})_2$ which is reached in a very large vessel. These maximum powers $(P_{max.})_1$ and $(P_{max.})_2$ are also equal to the maximum power $(P_{max.})$ attained by the fully baffled condition or by the off centered condition.

The detailed discussion will be published in a succeeding report.

III. Relations between the paddle width and the power consumption.

In the explanations given above, the authors considered that the areas relating to the power should be equal to bl_c for convenience' sake, but in reality, the following consideration may be more correct as is clear from Fig. 8. The liquid flow will be confined in the corner of paddles as shown by the hatched areas (A_1) (A_2) (A_3) for low and (B_1) (B_2) (B_3) for relatively high viscosity liquid.

Fig. 9 shows the increased ratio of the power consumed by the paddles having various width b to that for a paddle having the width $b=0.2D$ as ordinate versus increase in paddle width as abscissa.

To illustrate, in a liquid of low viscosity such as water, the radius r_c of the cylindrically rotating zone is large and l_c is small. If the liquid flows across the four corners of a paddle, the power will increase with the increases in paddle width until b reaches $2l_c$, but the rise in power will substantially stop when b becomes greater than $2l_c$ as shown in (A_3) in Fig. 8. Strictly speaking, the radius of the cylindrically rotating zone may vary with increase in the paddle width, but for simplicity of explanation the assumption that r_c is constant may be accepted, which will not cause serious errors. This estimation agrees well with the observed results as shown by curve (1) in Fig. 9 indicating that the power reaches substantially maximum when $b=2l_c$, i. e., at relatively small width. The length of l_c was calculated by equation (16) in this case.

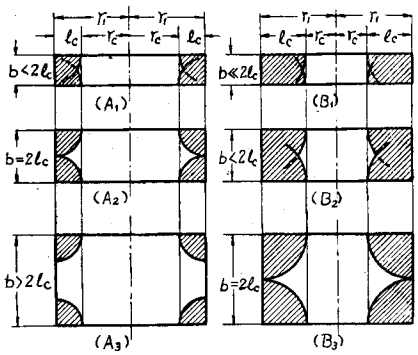

Fig. 8. Power Consumption for Liquids of Various Viscosities.

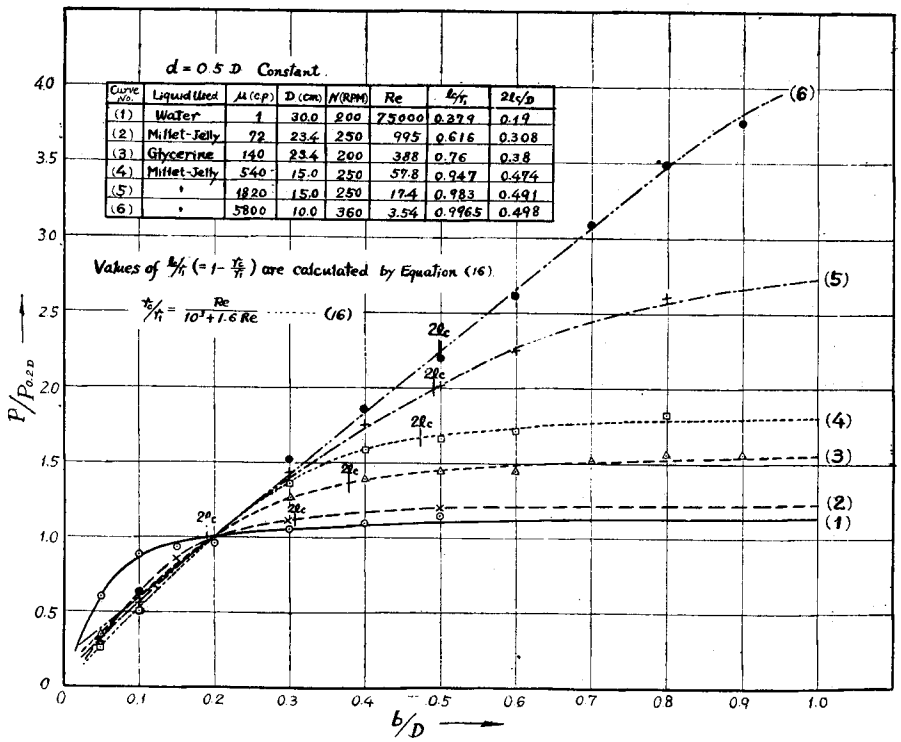

Fig. 9. Diagram Showing Power Increase Accompanied by Increases in Paddle Width.

On the other hand, in a liquid of relatively high viscosity the cylindrically rotating zone becomes smaller so that the limit of the increases in power with the increases in paddle width will shift to the side of larger paddle width as shown by (B_1) (B_2) (B_3) in Fig. 8 and by curve (2) and (3) in Fig. 9.

Finally, in a highly viscous liquid whose viscosity is greater than 5 poises shown by curve (4), r_c tends to zero and l_c to r_1. The power continues to increase with the increase in paddle width until b reaches $2l_c(=2r_1=d)$. And the power for paddles having width b greater than d becomes substantially constant. This is a maximum viscosity region for turbulent state. Curve (5) shows the result of experiments in a liquid having viscosity of 18.2 poises and is in a transitional range from turbulent to laminar flow.

Power continues to increase somewhat for paddles having width b greater than d. Curve (6) shows the results of experiments using a liquid whose viscosity is 58 poises, and is in the state of perfectly laminar flow so that power continues to increrse linearly with the increase in width b even in the range of b greater than d.

J. H. Rushton stated in the "Unit Operation Review" in 1953 (On Mixing) that "paddle impellers used in the United States have ratios of blade length (One-half of impeller diameter) to blade width of approximately 3 to 1 and 4 to 1, whereas the German practice is in the neighborhood of 1 to 2 and 1 to 3".

From the results the authors have gained, it is reasonable to choose the paddle width according to the viscosity of liquid to be agitated, namely, for liquids of low viscosity, paddles of small width will be efficient and for liquids of high viscosity, paddles of large width (and long span) are extremely effective.

Further details will be presented on a succeeding report.

Notations

r_2 : Radius of vessel
D : Diameter of vessel $=2r_2$
H : Static liquid depth
r_1 : Paddle radius
d : Paddle diameter $=2r_1$
b : Paddle width
r_c : Radius of cylindrically rotating zone (forced vortex zone)
l_c : r_1-r_c
ω : Angular velocity of paddle, radian/sec.
n : Agitator speed, rev./sec.
y : r_c/r_2
z : Height of liquid surface from bottom, shown in Fig. 1a.

V : Total Liquid volume charged in a vessel

m : Mass of liquid element

f : Resisting force

u_r : Relative velocity of paddle and liquid flow

$P_{max.}$: Maximum power consumed by paddle.

μ : Viscosity of liquid

ρ : Density of liquid

K, K', K'', c, c': Proportionality constants.

Literature Cited

1) S. Nagata, N. Yoshioka and T. Yokoyama: Chem. Eng. and Chemical Apparatus (Japan) Vol. 8, 43 (1950).
2) V. L. Streeter: Fluid Dynamics, 204 (1948) McGraw-Hill Book Co.
3) S. Tomochika: Fluid Dynamics, 248 (1940) Kyōritsu-sha (Japan).
4) O. Miyagi: Mechanical Engineering (Japan), **35**, 177, 197 (1932).
5) S. Nagata, T. Yokoyama and T. Saitō, Chem. Eng. (Japan), **18**, 228 (1954).